

Crystal-field effects of Sm^{3+} ions in $\text{Sm}_2\text{Fe}_{17}\text{N}_x$

T. S. Zhao

Department of Physics, Jilin University, Changchun 130023, People's Republic of China

X. C. Kou

Institute of Metal Research, Academia Sinica, Shenyang 110015, People's Republic of China

R. Grössinger and H. R. Kirchmayr

Institute of Experimental Physics, Technical University of Vienna, Wien, Austria

(Received 11 April 1991)

Using only two crystalline electric-field parameters A_2^0 and A_4^0 and the Sm-Fe exchange field H_{ex} , the magnetic-anisotropy behavior of the Sm ion in $\text{Sm}_2\text{Fe}_{17}\text{N}_x$ is described. It is shown that a field-induced noncollinear coupling between the spin and orbital moments of the Sm ion takes place during the magnetization process when the external field is applied along the hard axis. This noncollinear coupling causes a very different magnetization process of the Sm moment at $T=0$ and 300 K.

$R_2\text{Fe}_{17}$ compounds (R represents the rare-earth elements) hold the highest saturation magnetization of all the binary R -Fe compounds. It is therefore reasonable to make efforts to use these compounds for producing permanent magnets. However none of these compounds displays a uniaxial anisotropy (which is indispensable for a permanent magnet) at or above room temperatures. This together with their rather low Curie temperature (being close to room temperature) has made all such efforts unsuccessful. It was recently found that introducing N as interstitial atoms in $R_2\text{Fe}_{17}$ compounds leads to a large improvement of their intrinsic magnetic properties.^{1,2} The N addition to $R_2\text{Fe}_{17}$ leads to an expansion of the crystal lattice which is accompanied by an increase of the saturation magnetization and the Curie temperature (about 400 K higher than that of the $R_2\text{Fe}_{17}$). The Fe-sublattice anisotropy of this nitride favors alignment along the basal plane in the entire magnetically ordered temperature range. A spin-reorientation transition, described as a change of the easy direction of magnetization from the c axis to the basal plane with increasing temperature, was found for $\text{Er}_2\text{Fe}_{17}\text{N}_x$ and $\text{Tm}_2\text{Fe}_{17}\text{N}_x$. The nature of this transition is due to a temperature-induced competition between the uniaxial Er- or Tm-sublattice anisotropy and the easy-plane Fe-sublattice anisotropy.^{3,4} Uniaxial anisotropy was found in $\text{Sm}_2\text{Fe}_{17}\text{N}_x$ over the entire ferromagnetic temperature range. The temperature dependence of the anisotropy field H_A of $\text{Sm}_2\text{Fe}_{17}\text{N}_x$ was measured above room temperature by using the singular point detection (SPD) technique.⁵ The value of H_A of $\text{Sm}_2\text{Fe}_{17}\text{N}_x$ at room temperature was predicted to be around 140 kOe.⁵ At 4.2 K, the high-field measurements on magnetically aligned powder $\text{Sm}_2\text{Fe}_{17}\text{N}_x$ showed that even at 350 kOe the saturation-magnetization state is not achieved when the field is applied perpendicular to the alignment direction.^{6,7} Additionally, a coercivity of 30 kOe (at room temperature) was developed for $\text{Sm}_2\text{Fe}_{17}\text{N}_x$ by using the mechanical-alloying technique and a subsequent two-step annealing process.⁸

The large uniaxial anisotropy in $\text{Sm}_2\text{Fe}_{17}\text{N}_x$ arises from

the Sm ion being subjected simultaneously to the crystalline electric field (CEF) and the Sm-Fe exchange field. In this paper, the two major CEF parameters A_2^0 and A_4^0 were determined to describe the large anisotropy of the Sm ion. Using these parameters, our calculation revealed a very different magnetization behavior of the Sm moment during the magnetization process along the hard axis at $T=0$ and 300 K.

$\text{Sm}_2\text{Fe}_{17}$ crystallizes in the $\text{Th}_2\text{Zn}_{17}$ structure. Introducing N as an interstitial atom causes no basic change of its crystallographic symmetry. In $\text{Sm}_2\text{Fe}_{17}\text{N}_x$, the Sm ions occupy the $6c$ site. In the presence of an external magnetic field \mathbf{H} , the Hamiltonian of the Sm ion can be expressed as

$$\mathcal{H} = \lambda \mathbf{L} \cdot \mathbf{S} + \mathcal{H}_{\text{CEF}} + 2\mu_B \mathbf{S} \cdot \mathbf{H}_{\text{ex}} + \mu_B (\mathbf{L} + 2\mathbf{S}) \cdot \mathbf{H}, \quad (1)$$

where λ is the spin-orbit coupling constant; \mathbf{L} and \mathbf{S} are the total orbital and spin angular momenta, respectively; \mathcal{H}_{CEF} is the CEF Hamiltonian; \mathbf{H}_{ex} is the exchange field acting on the $4f$ spin from the Fe sublattice.

For Sm^{3+} ion, the sixth-order Stevens coefficient γ_J is zero for the ground-state $J = \frac{5}{2}$ multiplet, and the diagonal A_6^0 term—through mixing of the excited multiplets—has a smaller influence on the uniaxial anisotropy than the A_4^0 term. Neglecting the off-diagonal and sixth-order CEF terms, the CEF Hamiltonian of the Sm ion in $\text{Sm}_2\text{Fe}_{17}\text{N}_x$ can be written as

$$\mathcal{H}_{\text{CEF}} = A_2^0 C_2^0 + A_4^0 C_4^0, \quad (2)$$

where A_n^0 and C_n^0 ($n=2,4$) are the CEF parameters and the tensor operators, respectively. The matrix elements of Eq. (1) have been calculated by using the irreducible-tensor operator technique.⁹ In this calculation the mixing of the excited ($J = \frac{7}{2}$ and $\frac{9}{2}$) multiplets of the Sm ion with $\lambda = 410$ K has been taken into account. The eigenvalues E_n and eigenfunctions $|n\rangle$ [$n=1,2,\dots,\sum_J(2J+1)=24$] are calculated by diagonalizing the 24×24 matrix of Eq. (1). The free energy $F(T, \mathbf{H}, \mathbf{H}_{\text{ex}})$ of the

$\text{Sm}_2\text{Fe}_{17}\text{N}_x$ system per formula unit can be obtained by

$$F(T, \mathbf{H}, \mathbf{H}_{\text{ex}}) = -2k_B T \ln Z + K_{\text{Fe}}^{\text{Fe}} \sin^2 \theta_{\text{Fe}} - \mathbf{M}_{\text{Fe}} \cdot \mathbf{H}, \quad (3)$$

$$Z = \sum_n \exp(-E_n/k_B T), \quad (4)$$

where $K_{\text{Fe}}^{\text{Fe}}$ and \mathbf{M}_{Fe} are the magnetic-anisotropy constant and the magnetic moment of the Fe sublattice per formula unit, respectively. The values of $K_{\text{Fe}}^{\text{Fe}}(T)/K_{\text{Fe}}^{\text{Fe}}(0)$ and $M_{\text{Fe}}(T)/M_{\text{Fe}}(0)$ are assumed to be the same as those of Y_2Fe_{17} after scaling the different Curie temperatures.¹⁰ From the magnetization curves of $\text{Y}_2\text{Fe}_{17}\text{N}_x$ measured parallel and perpendicular to the alignment direction at 4.2 K,⁶ the value of $K_{\text{Fe}}^{\text{Fe}}(0)$ has been estimated to be -52 K/f.u. (corresponding to the anisotropy field of 40 kOe). The value for $M_{\text{Fe}}(0)$ is taken to be $39\mu_B/\text{f.u.}$ $\mathbf{H}_{\text{ex}}(T)$ is assumed to be proportional to and antiparallel to $\mathbf{M}_{\text{Fe}}(T)$. Using the molecular coefficient $n_{\text{Sm-Fe}}$ of $\text{Sm}_2\text{Fe}_{17}$ derived from an analysis of the Curie temperature,¹¹ the value of $\mu_B H_{\text{ex}}(0)$ in $\text{Sm}_2\text{Fe}_{17}\text{N}_x$ has been calculated to be 300 K.

The equilibrium direction of \mathbf{M}_{Fe} , for given applied external field \mathbf{H} and temperature T , can be determined by minimizing the free energy $F(T, \mathbf{H}, \mathbf{H}_{\text{ex}})$. The magnetic moment of the Sm ion is given by

$$\mathbf{M}_{\text{Sm}} = \mathbf{M}_{\text{Sm}}^L + \mathbf{M}_{\text{Sm}}^S, \quad (5)$$

where \mathbf{M}_{Sm}^L and \mathbf{M}_{Sm}^S are the orbital moment and spin moment of the Sm ion, respectively, and can be calculated as

$$\mathbf{M}_{\text{Sm}}^L = - \sum_n \mu_B \langle n | \mathbf{L} | n \rangle \frac{\exp(-E_n/k_B T)}{Z}, \quad (6)$$

$$\mathbf{M}_{\text{Sm}}^S = - \sum_n \mu_B \langle n | 2\mathbf{S} | n \rangle \frac{\exp(-E_n/k_B T)}{Z}. \quad (7)$$

The total magnetic moment \mathbf{M} of the system can be obtained by

$$\mathbf{M} = 2\mathbf{M}_{\text{Sm}} + \mathbf{M}_{\text{Fe}}. \quad (8)$$

The CEF parameters used in the present calculation are $A_2^0 = -340$ K and $A_4^0 = 200$ K. Using these parameters and the exchange field $\mu_B H_{\text{ex}} = 300$ K, the calculated magnetization curves at $T=0$ and 300 K for $\text{Sm}_2\text{Fe}_{17}\text{N}_x$ are shown in Fig. 1. Since single crystal $\text{Sm}_2\text{Fe}_{17}\text{N}_x$ is not yet available, the experimental data of the magnetization measured on magnetically aligned powder $\text{Sm}_2\text{Fe}_{17}\text{N}_x$ are also shown in Fig. 1.^{6,12} The calculated anisotropy fields H_A of $\text{Sm}_2\text{Fe}_{17}\text{N}_x$ are 312 and 137 kOe at $T=0$ and 300 K, respectively. The broken lines presented in Fig. 1 indicate the calculation when the external field \mathbf{H} makes an angle of 85° with the c axis. In this case, it is evident that even at the external field of 400 kOe the saturation magnetization state is still not achieved. This gives an explanation of the fact that the saturation magnetization state with the external field applied perpendicular to the alignment direction of $\text{Sm}_2\text{Fe}_{17}\text{N}_x$ is still not achieved at 350 kOe.^{6,7} At 300 K, similar behavior is found. If the external field \mathbf{H} makes an angle of 85° with the c axis, even at fields as high as 200 kOe (about 60 kOe higher than the anisotropy field) the Fe-sublattice moment is still located at 60° with respect to the c axis. The calculated temperature dependence of the anisotropy field H_A is

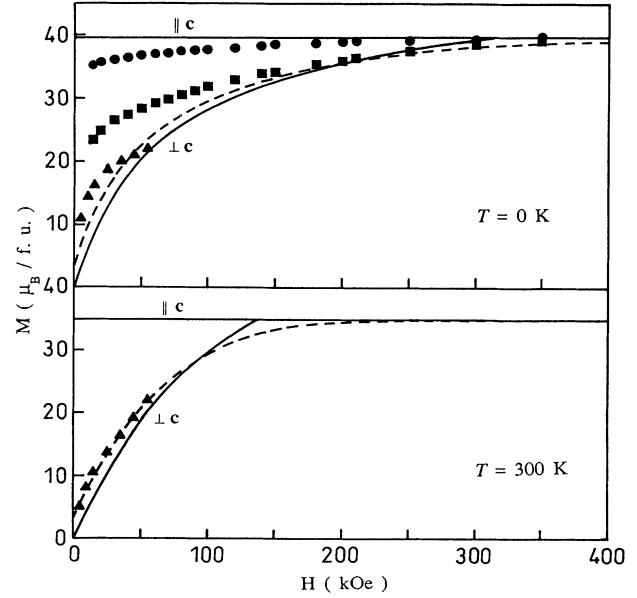


FIG. 1. The calculated and experimental magnetization curves parallel and perpendicular to the c axis for $\text{Sm}_2\text{Fe}_{17}\text{N}_x$. The solid lines represent the calculation; the dashed lines represent the calculation with the applied field making an angle of 85° with the c axis. The experimental data are taken from Ref. 6 (●, ■) and Ref. 12 (▲).

shown in Fig. 2. For comparison, the experimental values of H_A determined by the SPD technique above room temperature are also presented.⁵ It can be seen that there is good agreement between calculation and experiment. The stabilization energy ΔF is the difference between the free energy of the Sm ion when \mathbf{H}_{ex} is applied along the hard axis and when it is applied along the c axis. ΔF has been calculated in the temperature range from 0 to 600 K and is shown in Fig. 3. The Fe-sublattice anisotropy energy ($-K_{\text{Fe}}^{\text{Fe}}$) is also presented in Fig. 3 for comparison. It follows from this figure that the stabilization energy of the Sm sublattice is much larger than that of the Fe sublat-

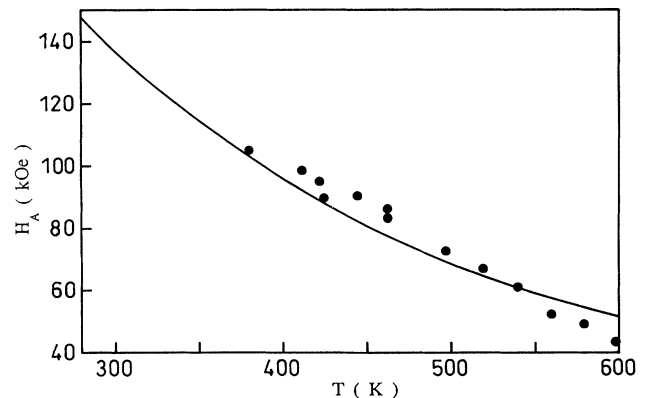


FIG. 2. The calculated and experimental temperature dependence of the anisotropy field H_A for $\text{Sm}_2\text{Fe}_{17}\text{N}_x$. (—), calculation; (●), experimental data (Ref. 5).

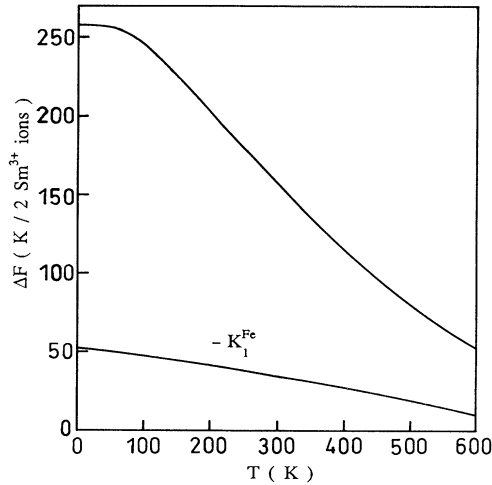


FIG. 3. The calculated stabilization energy ΔF of the Sm ion and the magnetic anisotropy constant $-K_1^{\text{Fe}}$ of the Fe sublattice as a function of temperature.

tion, which explains why there is no spin-reorientation transition in $\text{Sm}_2\text{Fe}_{17}\text{N}_x$. This large stabilization energy of the Sm sublattice is the source of the large anisotropy field of $\text{Sm}_2\text{Fe}_{17}\text{N}_x$.

The calculated temperature dependence of M_{Sm} , M_{Sm}^L , and M_{Sm}^S is illustrated in Fig. 4. The calculated values of M_{Sm} are $0.308\mu_B$ and $0.048\mu_B$ at $T=0$ and 300 K, respectively. The crossover temperature T_{co} , at which the total Sm moment becomes zero, is found to be 337 K. The dashed lines presented in the figure indicate the cal-

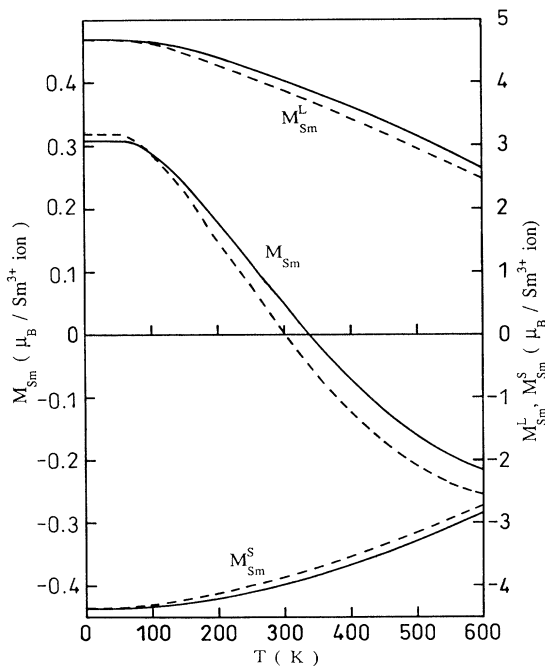


FIG. 4. The calculated M_{Sm} , M_{Sm}^L , and M_{Sm}^S as a function of temperature. The dashed lines represent the calculation not including the CEF interaction.

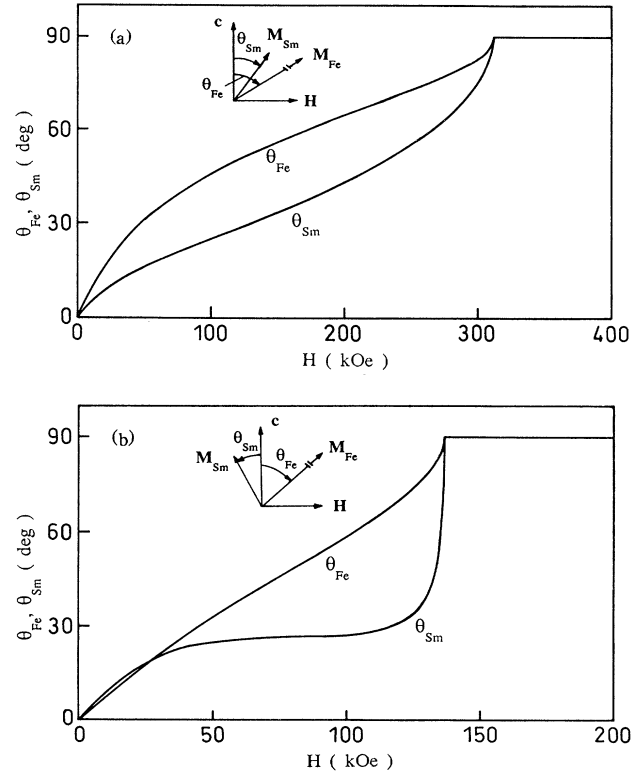


FIG. 5. The field dependence of the angles θ_{Fe} and θ_{Sm} during the magnetization process along the hard axis at (a) $T=0$ K and (b) 300 K.

culations that did not take the CEF interaction into account. It follows from this figure that if the CEF interaction is neglected in the calculation, T_{co} decreases to 301 K. This fact suggests clearly that the CEF interaction makes a remarkable increase in the crossover temperature.

Figures 5(a) and 5(b) show the magnetic-field dependence of the angles θ_{Fe} and θ_{Sm} for $\text{Sm}_2\text{Fe}_{17}\text{N}_x$ during the magnetization process with the field applied perpendicular to the c axis at $T=0$ and 300 K, respectively. For the exact definition of θ_{Fe} and θ_{Sm} , see the figures. At $T=0$ K, \mathbf{M}_{Sm} and \mathbf{M}_{Fe} rotate toward the \mathbf{H} direction continuously, but not collinearly, with increase of the external field. The maximum angle between two moments becomes as high as $\Delta\theta = \theta_{\text{Fe}} - \theta_{\text{Sm}} = 22.6^\circ$ at 155 kOe. At $T=300$ K, a very different magnetization process of \mathbf{M}_{Sm} is found. With increasing external field, \mathbf{M}_{Sm} rotates toward the direction antiparallel to \mathbf{H} rather than toward \mathbf{H} as at $T=0$ K. The pronounced noncollinear arrangement between \mathbf{M}_{Sm} and \mathbf{M}_{Fe} at $T=0$ K and the different magnetization process of \mathbf{M}_{Sm} at $T=0$ and 300 K are caused by the field-induced noncollinear coupling between \mathbf{M}_{Sm}^L and \mathbf{M}_{Sm}^S . Because of the weak L-S coupling of the Sm ion, a noncollinear coupling between \mathbf{M}_{Sm}^L and \mathbf{M}_{Sm}^S will occur under the strongly combined action of the CEF, the exchange field and the external field. The maximum angle between \mathbf{M}_{Sm}^L and $-\mathbf{M}_{\text{Sm}}^S$ reaches as high as about 1° . Figure 6 illustrates the variation of the magnetic struc-

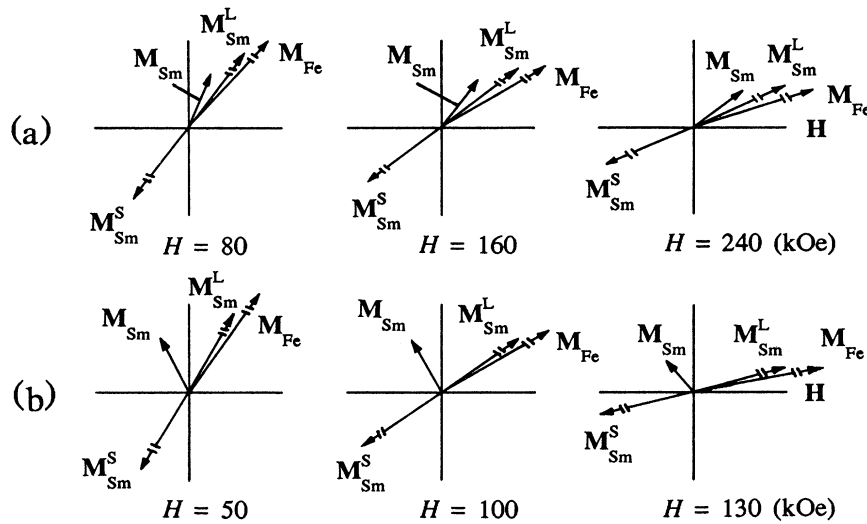


FIG. 6. The magnetic structures of $\text{Sm}_2\text{Fe}_{17}\text{N}_x$ at different field strengths during the magnetization process along the hard axis at (a) $T=0$ K and (b) 300 K.

tures of $\text{Sm}_2\text{Fe}_{17}\text{N}_x$ at (a) $T=0$ K and (b) 300 K. At $T=0$ K, due to the fact that M_{Sm}^L is always larger than M_{Sm}^S ($M_{\text{Sm}}^L - M_{\text{Sm}}^S \sim 0.3\mu_B$), the total Sm moment \mathbf{M}_{Sm} is closer to \mathbf{M}_{Sm}^L than \mathbf{M}_{Sm}^S , and is located in the region marked by the c axis and \mathbf{H} [see Fig. 6(a)]. At $T=300$ K, however, the values of M_{Sm}^L and M_{Sm}^S are nearly equal ($|M_{\text{Sm}}^L - M_{\text{Sm}}^S| < 0.05\mu_B$), resulting in a fact that the to-

tal Sm moment \mathbf{M}_{Sm} is located in the region marked by the c axis and $-\mathbf{H}$ [see Fig. 6(b)]. Additionally, the values of M_{Sm}^L and M_{Sm}^S vary with the external field such that M_{Sm}^S becomes larger than M_{Sm}^L when $H > 112$ kOe. Therefore \mathbf{M}_{Sm} rotates rapidly toward \mathbf{M}_{Sm}^S when $H > 112$ kOe and, finally, becomes antiparallel to \mathbf{H} when $H \geq H_A$.

- ¹J. M. D. Coey and H. Sun, *J. Magn. Magn. Mater.* **87**, L251 (1990).
- ²H. Sun, J. M. D. Coey, Y. Otani, and D. P. F. Hurley, *J. Phys. Condens. Matter* **2**, 6465 (1990).
- ³Bo-Ping Hu, Hong-Shuo Li, Hong Sun, J. F. Lawler, and J. M. D. Coey, *Solid State Commun.* **76**, 587 (1990).
- ⁴X. C. Kou, R. Grössinger, M. Katter, J. Wecker, L. Schultz, T. H. Jacobs, and K. H. J. Buschow, *J. Appl. Phys.* (to be published).
- ⁵M. Katter, J. Wecker, L. Schultz, and R. Grössinger, *J. Magn. Magn. Mater.* **92**, L14 (1990).
- ⁶J. P. Liu, K. Bakker, F. R. de Boer, T. H. Jacobs, and K. H. J. Buschow, *J. Less-Common Met.* (to be published).
- ⁷X. C. Kou, R. Grössinger, X. Li, P. Liu, F. R. de Boer, M. Katter, J. Wecker, L. Schultz, T. H. Jacobs, and K. H. J.

Buschow, *J. Appl. Phys.* (to be published).

- ⁸K. Schnitzke, L. Schultz, J. Wecker, and M. Katter, *Appl. Phys. Lett.* **57**, 2853 (1990).
- ⁹B. G. Wybourne, *Spectroscopic Properties of Rare Earth* (Interscience, New York, 1965).
- ¹⁰S. Sinnema, Ph.D. thesis, University of Amsterdam, 1988 (unpublished).
- ¹¹E. Belorizky, M. A. Fremy, J. P. Gavigan, D. Givord, and H. S. Li, *J. Appl. Phys.* **61**, 3971 (1987).
- ¹²Y. Z. Wang, G. C. Hadjipanayis, and D. J. Sellmyer, in *Proceedings of the Sixth International Symposium on Magnetic Anisotropy and Coercivity in Rare Earth-Transition Metal Alloys*, edited by S. G. Sankar (Carnegie Mellon Univ., Pittsburgh, Pennsylvania, 1990), p. 181.